An overview of the effect of large-scale inhomogeneities on small-scale turbulence[a)]

L. Danaila
L.E.T., University of Poitiers, 40 Av. du Recteur Pineau, 86022, Poitiers, France

F. Anselmet
I.R.P.H.E., 49 Rue F. Joliot-Curie, B.P. 146, 13388 Marseille Cedex 13, France

R. A. Antonia
Department of Mechanical Engineering, University of Newcastle, Newcastle, New South Wales 2308, Australia

(Received 12 June 2001; accepted 13 February 2002; published 5 June 2002)

The well-known isotropic relations [see Kolmogorov, Dokl. Akad. Nauk. SSSR **30**, 301 (1941); **32**, 16 (1941); A. M. Yaglom, *ibid.* **69**, 743 (1949)] between second-order and third-order structure functions are, in general, unlikely to be satisfied in turbulent flows encountered in the laboratory at moderate values of the Reynolds number. The main reason for this is the non-negligible correlation between the length scales at which the initial injection of turbulent energy occurs, those which dominate the transfer of this energy down the ''cascade'' and those which are responsible for dissipating this energy. In the majority of flows, there is a non-negligible inhomogeneity (sometimes nonstationarity) which may be caused by different physical phenomena. This paper presents an overview of how the equations of Kolmogorov and Yaglom can be ''generalized'' to provide a more realistic description of small-scale turbulence. The focus is mainly on locally isotropic regions of the flow, investigated using one-point measurements and Taylor's hypothesis. We are concerned principally with decaying grid turbulence, for which several results have already been obtained, but other flows, e.g., fully developed channel and jet flows, are also discussed. [DOI: 10.1063/1.1476300]

I. INTRODUCTION

In 1941, Kolmogorov[1,2] developed a relationship between the second-order moment of the longitudinal velocity increment over an interval r in the longitudinal (x_1) direction, $\langle(\Delta u_1)^2\rangle$, and the third-order moment, $\langle(\Delta u_1)^3\rangle$, also in the longitudinal direction. Here, u_1 is the component of the velocity fluctuation in the streamwise (i.e., longitudinal) direction and $\Delta u_1(r)=u_1(x_1+r)-u_1(x_1)$. This relation, often referred to as Kolmogorov's ''four-fifths law,'' when the effect of viscosity is negligible, is given by

$$-\langle(\Delta u_1)^3\rangle+6\nu\frac{d}{dr}\langle(\Delta u_1)^2\rangle=\tfrac{4}{5}\langle\epsilon\rangle r, \tag{1}$$

where the mean energy dissipation rate $\langle\epsilon\rangle$ is defined as

$$\langle\epsilon\rangle=\frac{1}{2}\nu\left\langle\left(\frac{\partial u_i}{\partial x_j}+\frac{\partial u_j}{\partial x_i}\right)^2\right\rangle. \tag{2}$$

Here, repeated indices indicate summation, ν is the kinematic viscosity of the fluid, u_i is the fluctuating velocity component in the ith direction, and angular brackets denote time averaging. Equation (1) is derived within the framework of Kolmogorov,[1,2] which assumes a cascade that is universal and locally isotropic for small enough scales and large enough Reynolds numbers.

In the same context of local isotropy, a similar relation was obtained by Yaglom[3] between the second-order moment of the temperature increment and the third-order mixed moment $\langle\Delta u_1(\Delta\theta)^2\rangle$:

$$-\langle\Delta u_1(\Delta\theta)^2\rangle+2\kappa\frac{d}{dr}\langle(\Delta\theta)^2\rangle=\tfrac{4}{3}\langle\epsilon_\theta\rangle r. \tag{3}$$

The rate of destruction of the scalar variance, $\langle\epsilon_\theta\rangle$, is defined as

$$\langle\epsilon_\theta\rangle\equiv\kappa\left\langle\left(\frac{\partial\theta}{\partial x_i}\right)\left(\frac{\partial\theta}{\partial x_i}\right)\right\rangle, \tag{4}$$

where κ is the molecular diffusivity of the scalar.

Kolmogorov's four-fifths law and Yaglom's four-thirds law have a cornerstone role in the study of turbulence since they are the simplest results derived from relations expressing conservations of momentum and heat, respectively, using homogeneity and local isotropy. Writing Eq. (1) as $A+B=C$, term C (directly proportional to $\langle\epsilon\rangle$), is associated with the transfer of energy at a scale r. Equation (1) indicates that, at scale r, the mean energy is transferred by both turbulent advection (term A) and molecular diffusion (term B). A similar interpretation applies to Yaglom's equation.

Equations (1) and (3) could also be used as alternate means of (experimentally) determining $\langle\epsilon\rangle$ and $\langle\epsilon_\theta\rangle$, since the second- and third-order moments could be inferred from

[a)]Presented at the Symposium in honor of John L. Lumley on his 70th birthday, Cornell University, June 2001.

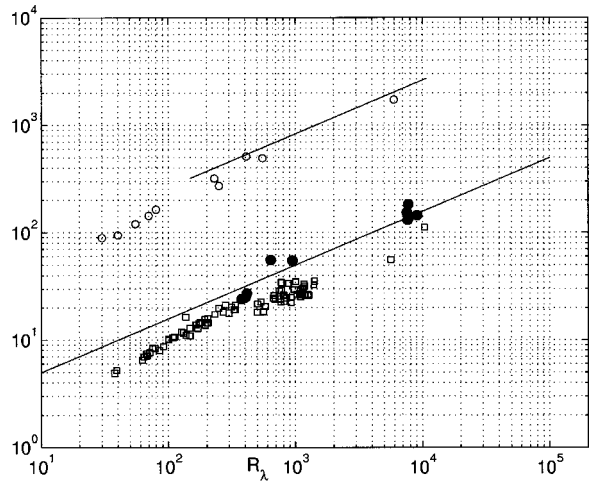

FIG. 1. R_λ dependence of values of $-\langle(\Delta u_1^*)^3\rangle$ and $-\langle\Delta u_1^*(\Delta\theta^*)^2\rangle$ for $r=\lambda$. (□) and (●) $-\langle(\Delta u_1^*)^3\rangle_{r=\lambda}$; solid line, Eq. (5); (○) $-\langle\Delta u_1^*(\Delta\theta^*)^2\rangle_{r=\lambda}$; solid line, Eq. (6). For clarity, the data for $-\langle\Delta u_1^*(\Delta\theta^*)^2\rangle_{r=\lambda}$ are shifted upward by a factor of 10. All these data are taken from Refs. 8 and 9.

hot- (and cold-) wire measurements, using Taylor's hypothesis and assuming local isotropy and homogeneity.

At small Reynolds numbers, the sum $A+B$ cannot be expected to balance C, except at the smallest scales (e.g., for grid turbulence, this equality is satisfied only for $r/\eta \lesssim 5$ at $R_\lambda = 66$[4]). We define $R_\lambda \equiv u_1'\lambda/\nu$, where u_1' is the root-mean-square longitudinal velocity fluctuation and $\lambda \equiv (\langle u_1^2\rangle/\langle(\partial u_1/\partial x_1)^2\rangle)^{1/2}$ is the longitudinal Taylor microscale. For intermediate Reynolds numbers ($100 < R_\lambda < 500$), Kolmogorov's four-fifths law and Yaglom's four-thirds law are not satisfied for moderate to large scales (e.g., Refs. 5–7). These equations are only satisfied up to a maximum separation which depends on the Reynolds number. Obviously, they cannot be verified at large r when the contributions from the two terms on the left-hand sides of Eqs. (1) and (3) become negligible.

A relatively simple means of quantifying the departure of available measurements from Eqs. (1) and (3) is to select a value of r which falls within the inertial range. If we identify r with λ and assume local isotropy, Eqs. (1) and (3) reduce to (the terms containing ν and κ are neglected)

$$-\langle(\Delta u_1^*)^3\rangle = \tfrac{4}{5}15^{1/4}R_\lambda^{1/2}, \tag{5}$$

$$-\langle\Delta u_1^*(\Delta\theta^*)^2\rangle = \tfrac{4}{3}15^{1/4}R_\lambda^{1/2}, \tag{6}$$

where the superscript asterisk indicates normalization by Kolmogorov temperature, velocity, and length scales. Experimental values for $-\langle(\Delta u_1^*)^3\rangle_{r=\lambda}$ and $-\langle\Delta u_1^*(\Delta\theta^*)^2\rangle_{r=\lambda}$ obtained in different flows are shown in Fig. 1.[8,9] Notwithstanding the scatter in the data, the magnitudes of these two quantities fall consistently below the estimates given by (5) and (6). The squares and closed circles in Fig. 1 are taken from Pearson and Antonia;[8] these data were obtained in a large assortment of flows (plane and circular jets, fully developed pipe and boundary layer flows including the atmospheric surface layer). The value $r=\lambda$ is expected to reside near the bottom end of the inertial range. When R_λ is small enough, the viscous/molecular diffusive contributions, viz. the second terms on the left-hand sides of (1) and (3), cannot be entirely neglected, which may partly explain the rather sharp fall off, below $R_\lambda \approx 500$, of the open squares and circles relative to the solid lines, viz. the right-hand sides of (1) and (3). Estimates of these contributions indicate however that they are insufficient to account for the shortfall between the theory (solid lines) and the experimental values of $-\langle(\Delta u_1^*)^3\rangle$ and $-\langle\Delta u_1^*(\Delta\theta^*)^2\rangle$. As will be seen in Secs. II and III, further contributions are required to restore the balance between the left- and right-hand sides of Eqs. (1) and (3) [at $r=\lambda$, these new contributions are expected to be comparable to the molecular contributions]. They are associated with the effect of large scale inhomogeneities which may differ intrinsically between different flows. Indeed, the difference may be such that, for the same R_λ, the inhomogeneous contributions may vary from flow to flow or possibly different regions of the same flow.

Experimentally, it may be impossible to generate homogeneous and isotropic turbulence. This goal is more likely to be within the reach of numerical simulations. Usually, the simulations of homogeneous and isotropic turbulence are forced to reach a statistically stationary state with a given energy dissipation rate (see Refs. 10 and 11, and references therein). The forcing is typically via a continuous injection of energy at low wave numbers, such that the energy introduced is equal to that dissipated. Under these conditions, the second-order structure functions then exhibit an approximate $r^{2/3}$ behavior over a range which increases as R_λ increases.[11] The simulations of Gotoh[12] at $R_\lambda \approx 390$ indicate that the distribution of $-\langle(\Delta u_1^*)^3\rangle$ is in closer—but not perfect—agreement with $4r^*/5$ than experimental data at comparable R_λ. The "imperfect" balance of Eq. (1) for the simulation may reflect the existing anisotropy at the large scales. The balance of Eq. (1) has also been investigated in Ref. 13 for globally isotropic turbulence ($R_\lambda \lesssim 142$). The 4/5th plateau is well-established even at these small Reynolds numbers. These authors solve the Navier–Stokes equations without any forcing, but impose symmetries on the flow. Alvelius[14] also used low wave number spectral forcing in a large eddy simulation of stationary homogeneous turbulence and concluded that the inertial range relation $-\langle(\Delta u_1)^3\rangle = 4/5\langle\epsilon\rangle r$ is satisfied only if R_λ is very large or, when R_λ is moderate, if a statistically steady state exists.

The agreement (or disagreement) of Kolmogorov's similarity hypothesis with reality has more traditionally been investigated spectrally. Phenomenologically, spectra are expected to exhibit a $k^{-5/3}$ behavior, i.e., an inertial range when the Reynolds number is sufficiently large. Thus, experiments and numerical simulations present spectra with a widening inertial range as R_λ increases.[6,7,10] The discrepancy between the "asymptotic" predictions of Kolmogorov and "reality" is the principal theme of this paper. Although derived from rigorous (Navier–Stokes and advection–diffusion) equations, Kolmogorov's and Yaglom's relations are generally not satisfied experimentally. Evidently, the majority of turbulent flows that we encounter include effects that are extraneous to Eqs. (1) and (3). In order to account for the role of the large scales, Frisch[15] added a random forcing term (acting only at

large scales) to Kolmogorov's equation. A detailed study of Kolmogorov's equation has been carried out by Hill.[16] The nonstationarity of decaying flows was analytically taken into account, although no quantitative verification was made. The influence of large scales on the statistical properties of the cascade has also been addressed by Moisy *et al.*[17] and by Lindborg[18] (who treats both a jet flow and grid turbulence in the same manner, using a nonstationary term estimated with the use of the $k-\epsilon$ model). Note also that his model cannot be utilized for studying the large-scale effect on small-scale intermittency, since the level of agreement obtained in the inertial range needs to be improved.

In order to better appreciate the imbalance of Eqs. (1) and (3) at large scales, it is appropriate to consider the limiting forms at small separations. The isotropic mean energy dissipation rate, $\langle\epsilon\rangle$, is given by

$$\langle\epsilon\rangle_{\mathrm{iso}}=15\nu\left\langle\left(\frac{\partial u_1}{\partial x_1}\right)^2\right\rangle. \tag{7}$$

Equation (7) is often used in experiments since the right-hand side is readily measured. If the assumption of isotropy is indeed valid, then $\langle\epsilon\rangle$ and $\langle\epsilon\rangle_{\mathrm{iso}}$ are equal. Hereafter, we will clearly differentiate between $\langle\epsilon\rangle$ and its isotropic form, $\langle\epsilon\rangle_{\mathrm{iso}}$, as in Eq. (7). Given that

$$\lim_{r\to 0} 6\nu\frac{d}{dr}\langle(\Delta u_1)^2\rangle=\lim_{r\to 0} 6\nu\frac{d}{dr}\left\langle\frac{(\Delta u_1)^2}{r^2}r^2\right\rangle$$
$$=6\nu\left\langle\left(\frac{\partial u_1}{\partial x_1}\right)^2\right\rangle\frac{d}{dr}(r^2)=\frac{4}{5}\langle\epsilon\rangle_{\mathrm{iso}}r, \tag{8}$$

Eq. (1) reduces to $B=C$ in the limit $r\to 0$. In this case, term A is two orders of magnitude smaller and therefore negligible. Consequently, at the smallest scales, Eq. (1) is consistent with $\langle\epsilon\rangle_{\mathrm{iso}}$. This result is expected since Kolmogorov's equation was derived assuming small scales isotropy. Alternatively, Kolmogorov's equation will be verified for very small scales if and only if $\langle\epsilon\rangle=\langle\epsilon\rangle_{\mathrm{iso}}$. Analytical derivations[19] and experimental results[20,21] indicate that, in the presence of a mean shear, the small-scale structure is not isotropic, so that $\langle\epsilon\rangle\neq\langle\epsilon\rangle_{\mathrm{iso}}$.

Similarly, Eq. (3) is consistent for very small scales with

$$\langle\epsilon_\theta\rangle_{\mathrm{iso}}\equiv 3\kappa\left\langle\left(\frac{\partial\theta}{\partial x_1}\right)^2\right\rangle. \tag{9}$$

Experimental and numerical studies have shown[7,22–25] that, in a turbulent flow with an imposed mean scalar gradient (**G**), the turbulent scalar field is anisotropic, even for the smallest scales and large R_λ. A relevant illustration of this anisotropy is the inequality between the temperature derivative variance in the direction parallel to **G** and that in other directions.[7,23,24] In particular, if one defines the x_3 direction as parallel to **G**, the variance of the scalar derivative along this direction is about 1.4 times larger than the variance of the derivative along a perpendicular direction.

Since Kolmogorov's equation is consistent at very small scales with $\langle\epsilon\rangle_{\mathrm{iso}}$, we consider here a more general version of Eq. (1), which leads to a less restrictive form of the mean energy dissipation rate. A more general relation between second- and third-order moments of velocity increments is given by[26]

$$-\langle\Delta u_1(\Delta u_i)^2\rangle+2\nu\frac{d}{dr}\langle(\Delta u_i)^2\rangle=\frac{4}{3}\langle\epsilon\rangle r. \tag{10}$$

The analogy between Eq. (10) and Yaglom's equation for temperature increments was also discussed in Ref. 26. This generalized form of Kolmogorov's equation presents the same pathology as Eqs. (1) and (3), i.e., it is balanced only for relatively small scales when the Reynolds number is moderate. The range over which Eq. (10) is verified is identical to that for Eq. (1).[26] Equation (10) actually represents an extended form (for all velocity components) of Kolmogorov's equation. For very small scales, it complies with the homogeneous form of $\langle\epsilon\rangle$, viz.

$$2\nu\lim_{r\to 0}\frac{d}{dr}\langle(\Delta u_i)^2\rangle=4\nu\left\langle\left(\frac{\partial u_i}{\partial x_1}\right)^2\right\rangle r$$
$$=\frac{4}{3}\langle\epsilon\rangle r$$
$$\Rightarrow\langle\epsilon\rangle=3\nu\left\langle\left(\frac{\partial u_i}{\partial x_1}\right)^2\right\rangle=\langle\epsilon\rangle_{\mathrm{hom}}. \tag{11}$$

Equation (10) will receive particular attention here, since its derivation from the Navier–Stokes equations has the same simplicity as the derivation of Eq. (3).

It seems apropos to comment on the subtle, if not intricate, role played by $\langle\epsilon\rangle$ and $\langle\epsilon_\theta\rangle$, given that these quantities relate both to the small scales and, at the same time, reflect information on the large scales. There is now significant evidence[27,28] to indicate that the dimensionless parameters $C_\epsilon\equiv\langle\epsilon\rangle L/u_1'^3$ and $C_{\epsilon_\theta}\equiv\langle\epsilon_\theta\rangle L/\langle\theta^2\rangle u_1'$ (L is the injection scale) depend on the Reynolds number, the nature of the flow, including initial conditions. ''Constant'' values of C_ϵ and C_{ϵ_θ} are obtained only when the previous effects disappear. The observed behavior of C_ϵ and C_{ϵ_θ} is consistent with the lack of a true inertial range and the imbalances measured for Eqs. (1) and (3) (e.g., Fig. 1). In answer to the question ''What part of modeling is in serious need of work?'' Lumley[29] points to ''the mechanism that sets the level of dissipation in a turbulent flow, particularly in changing circumstances.'' He goes on to say that, for a steady flow, the level is determined by the rate at which the turbulent kinetic energy enters the spectral pipeline. At sufficiently high R_λ, one expects a range of wave numbers in which neither production nor dissipation of energy occurs so that the energy is conserved and simply passes from wave number to wave number. This classical scenario would be perturbed if the flow is nonstationary or inhomogeneous; the consequent spectral ''leakage'' would be further accentuated as R_λ decreases.

The paper is organized as follows. Following presentation of the theoretical framework, as developed mainly for the velocity field (Sec. II), we recall results previously published in slightly heated decaying turbulence[4] (Sec. III) and on the centerline of a plane channel flow[30] (Sec. IV). How-

ever, most of the results will be for decaying grid turbulence, arguably the simplest turbulent flow that can be investigated in the laboratory. It is appropriate, in the context of this particular edition of Physics of Fluids, to acknowledge the contributions of John Lumley and Zellman Warhaft to the study of the decay of temperature fluctuations in grid turbulence.[7,23,31,32]

II. THEORETICAL CONSIDERATIONS

Our major objective is to gain some insight into the flow physics which results in an imbalance between the left- and right-hand sides of Eqs. (1), (3), and (10), in different flows. We are particularly concerned with (slightly heated) decaying grid turbulence and the centerline of a fully developed channel flow. A turbulent grid flow is characterized by a streamwise inhomogeneity reflected in the decay in the x_1 direction of quantities such as the turbulent kinetic energy $\langle q^2\rangle=\langle(u_iu_i)\rangle/2$, temperature variance $\langle\theta^2\rangle$, as well as the dissipation rates $\langle\epsilon\rangle$ and $\langle\epsilon_\theta\rangle$. To date, this flow has not been simulated numerically, although there have been many direct numerical as well as large eddy simulations of decaying box turbulence. In this case, the flow is homogeneous but nonstationary, as reflected in the temporal evolution of $\langle q^2\rangle$, $\langle\theta^2\rangle$, $\langle\epsilon\rangle$, and $\langle\epsilon_\theta\rangle$.

In a fully developed channel flow, there is no decay in the streamwise direction but, in this case, the inhomogeneity is associated with a large-scale diffusion of energy across the centerline.

The inhomogeneities of grid and channel flow turbulence are taken into account in our derivations, although local isotropy is still maintained for all the other (turbulent advection, molecular diffusion, and pressure diffusion) terms. From a mathematical point of view, the extra inhomogeneous terms are introduced and manipulated within a quasi-isotropic context. This issue is discussed later in this section. Here, we recall briefly the salient steps in deriving the generalized form of Kolmogorov's equation (10).[26]

Using the same procedure as presented in Refs. 16, 30, and 33 we write the incompressible Navier–Stokes equations at the two points $\mathbf{x}$ and $\mathbf{x}^+$, which are separated by the increment $\mathbf{r}=\mathbf{x}^+-\mathbf{x}$, viz.

$$\partial_t u_i+u_\alpha\partial_\alpha u_i=-\partial_i p/\rho+\nu\partial_\alpha^2 u_i, \tag{12}$$

$$\partial_t u_i^++u_\alpha^+\partial_\alpha^+ u_i^+=-\partial_i^+ p^+/\rho+\nu\partial_\alpha^{2+}u_i^+. \tag{13}$$

The superscript + refers to $\mathbf{x}^+$, and ρ is the fluid density. In (12) and (13), u_i is the instantaneous velocity vector, with $\langle u_i\rangle=U_1\delta_{i1}$ (δ_{ij} is the Kronecker symbol, U_1 is the mean velocity); p is the instantaneous pressure, $\partial_t\equiv\partial/\partial t$, $\partial_\alpha\equiv\partial/\partial x_\alpha$, and ∂_α^2 is the Laplacian $\partial^2/\partial x_\alpha^2$ (hereafter, the notation ∂_α and ∂_α^+ will be used to denote derivatives with respect to x_α and x_α^+; when other spatial variables are involved, the derivatives will be written explicitly, e.g., $\partial/\partial r$ or $\partial/\partial X_\alpha$). Note here that we address only flows where the mean velocity has only one component U_1, e.g., grid turbulence and channel flow. In a round jet, a slightly more general treatment is needed; this will not be pursued here. We then consider that the two points $\mathbf{x}$ and $\mathbf{x}^+$ are independent, i.e., u_i depends only on $\mathbf{x}$ and u_i^+ depends only on $\mathbf{x}^+$, so that subtraction of (12) from (13) yields an equation for the velocity increment $\Delta u_i=u_i^+-u_i$, viz.

$$\partial_t(\Delta u_i)+U_1\partial_1(\Delta u_i)+u_\alpha^+\partial_\alpha^+(\Delta u_i)+u_\alpha\partial_\alpha(\Delta u_i)$$
$$=-(\partial_i+\partial_i^+)(\Delta p)/\rho+\nu(\partial_\alpha^2+\partial_\alpha^{2+})(\Delta u_i). \tag{14}$$

Hereafter, for simplicity, u_i will denote the fluctuating velocity (i.e. $\langle u_i\rangle=0$).

By subtracting and adding the term $u_\alpha\partial_\alpha^+(\Delta u_i)$ to the left-hand side of (14),

$$\partial_t(\Delta u_i)+U_1\partial_1(\Delta u_i)+\Delta(u_\alpha)\partial_\alpha^+(\Delta u_i)$$
$$+u_\alpha\partial_\alpha^+(\Delta u_i)+u_\alpha\partial_\alpha(\Delta u_i)$$
$$=-(\partial_i+\partial_i^+)(\Delta p)/\rho+\nu(\partial_\alpha^2+\partial_\alpha^{2+})(\Delta u_i). \tag{15}$$

We take into account the small local inhomogeneity by also considering the derivative with respect to the midpoint,[16] i.e.,

$$\mathbf{X}=\tfrac{1}{2}(\mathbf{x}+\mathbf{x}^+). \tag{16}$$

Thus,

$$\partial_\alpha^+\equiv\frac{\partial}{\partial r_\alpha}+\frac{1}{2}\frac{\partial}{\partial X_\alpha}, \tag{17}$$

$$\partial_\alpha\equiv-\frac{\partial}{\partial r_\alpha}+\frac{1}{2}\frac{\partial}{\partial X_\alpha}, \tag{18}$$

resulting in $\partial/\partial X_\alpha=\partial_\alpha+\partial_\alpha^+$. Note that relation (17) applies to both fluctuating and averaged quantities. The new derivative simply reflects the local inhomogeneity of the considered scale r, i.e., the extended effect of the very large (injection) scales on the considered scale. By using (17) we then have

$$\Delta(u_\alpha)\partial_\alpha^+(\Delta u_i)=\Delta(u_\alpha)\frac{\partial(\Delta u_i)}{\partial r_\alpha}+\frac{1}{2}\Delta(u_\alpha)\frac{\partial}{\partial X_\alpha}(\Delta u_i). \tag{19}$$

By taking (19) into account and by multiplying Eq. (15) with $2\Delta u_i$ and averaging, we finally obtain

$$(\partial_t+U_1\partial_1)\langle(\Delta u_i)^2\rangle(\mathbf{r})+\left(\frac{\partial}{\partial r_\alpha}+\frac{1}{2}\frac{\partial}{\partial X_\alpha}\right)\langle\Delta(u_\alpha)(\Delta u_i)^2\rangle(\mathbf{r})$$
$$+[\partial_\alpha^+ +\partial_\alpha]\langle u_\alpha(\Delta u_i)^2\rangle(\mathbf{r})$$
$$=-2(\partial_i+\partial_i^+)\langle\Delta p\cdot\Delta u_i\rangle(\mathbf{r})$$
$$+2\nu\langle\Delta u_i(\partial_\alpha^2+\partial_\alpha^{2+})(\Delta u_i)\rangle(\mathbf{r}). \tag{20}$$

In obtaining Eq. (20), no particular hypothesis regarding the flow has been made; note that each term depends on the spatial vector $\mathbf{r}$. Relation (17) can be written for a flow with a characteristic inhomogeneity, for example a fully developed channel flow (not necessarily on the axis). We take x_3 in the direction normal to the wall. As long as the statistics are evaluated from one-point measurements using Taylor's hypothesis, the inhomogeneity of this flow at both $\mathbf{x}$ and $\mathbf{x}^+$ is along x_3. It follows that, $\partial_\alpha\langle\cdot\rangle=\partial_\alpha^+\langle\cdot\rangle=\partial_3\langle\cdot\rangle$ and relation (17), when applied to "averaged" quantities, becomes

$$\partial_\alpha^+\langle\cdot\rangle \equiv \frac{\partial}{\partial r_\alpha}\langle\cdot\rangle + \frac{1}{2}\frac{\partial}{\partial X_\alpha}\langle\cdot\rangle = \frac{\partial}{\partial r_\alpha}\langle\cdot\rangle + \partial_3\langle\cdot\rangle. \tag{21}$$

Under these conditions, and after applying relations (17) and (21) to the viscous term, Eq. (20) becomes

$$\begin{aligned}(\partial_t + U_1\partial_1)\langle(\Delta u_i)^2\rangle(\mathbf{r}) &+ \frac{\partial}{\partial r_\alpha}\langle\Delta(u_\alpha)(\Delta u_i)^2\rangle(\mathbf{r}) \\ &+ \partial_3\langle(u_3+u_3^+)(\Delta u_i)^2\rangle(\mathbf{r}) \\ &= -2(\partial_i+\partial_i^+)\langle\Delta p\cdot\Delta u_i\rangle(\mathbf{r}) \\ &\quad + 2\nu\left[\frac{\partial^2}{\partial r_\alpha{}^2} + \partial_3^2\right]\langle(\Delta u_i)^2\rangle(\mathbf{r}) - 4\langle\epsilon\rangle. \end{aligned} \tag{22}$$

We shall only consider the effect of the inhomogeneity on the ''inertial'' term A, via relation (19), and we simply neglect the term $\partial_3^2\langle(\Delta u_i)^2\rangle$ in Eq. (22). Our first hypothesis is to assume local isotropy for those terms which are present in a restricted scaling range (RSR) only, i.e., for the molecular diffusion and the advection terms. These terms exist only at small and moderate scales and depend therefore on r (the modulus of the separation $\mathbf{r}$) only. The divergence and Laplacian operators assume particular forms. Note that exactly the same assumptions are made in the classical equations (1), (3), or (10). The pressure-containing term is written as

$$\Pi = -2(\partial_i+\partial_i^+)\langle\Delta p\cdot\Delta u_i\rangle(\mathbf{r}) \propto \partial_3\langle\Delta p\Delta u_3\rangle(\mathbf{r}). \tag{23}$$

For large separations, $\Pi \to 4\partial_3\langle p u_3\rangle$, which is negligible in a channel flow,[30,34,35] not only on the axis, but everywhere. It is then reasonable to neglect Π.

We now turn our attention to the spatial dependence of the new terms in Eq. (22). The decay term $U_1\partial_1\langle(\Delta u_i)^2\rangle(\mathbf{r})$ depends on the second-order structure function $\langle(\Delta u_i)^2\rangle(\mathbf{r})$.

We will show that

$$U_1\partial_1\langle(\Delta u_i)^2\rangle(r_1) \approx U_1\partial_1\langle(\Delta u_i)^2\rangle(r_3), \tag{24}$$

which is equivalent to $\langle(\Delta u_i)^2\rangle(r_1)\approx\langle(\Delta u_i)^2\rangle(r_3)$. The validation of this approximation requires numerical investigations or rather special experimental measurements. For small scales, local isotropy requires that

$$\langle(\partial_1 u_i)(\partial_1 u_i)\rangle \approx \langle(\partial_3 u_i)(\partial_3 u_i)\rangle. \tag{25}$$

Relation (25) only holds in locally isotropic regions of the flow. Therefore, our analysis is well-adapted to locally isotropic regions of the flow, for instance, in grid turbulence and near the centerline of the channel flow. The large scale behavior of the second-order structure function is given by

$$\lim_{\mathbf{r}\to\infty}\langle(\Delta u_i)^2\rangle(\mathbf{r}) = \langle u_i^2\rangle(\mathbf{x}) + \langle u_i^2\rangle(\mathbf{x}+\mathbf{r}). \tag{26}$$

We need to recognize that when second-order structure functions are estimated from one-point measurements and Taylor's hypothesis, the points $\mathbf{x}$ and $\mathbf{x}^+$ are inferred from data at different times but at the same spatial location. Taylor's hypothesis thus ''simulates'' spatially homogeneous turbulence even though this state does not exist in reality. Under these particular conditions, Eq. (26) becomes

$$\lim_{\mathbf{r}\to\infty}\langle(\Delta u_i)^2\rangle(\mathbf{r}) = \langle u_i^2\rangle(\mathbf{x}) + \langle u_i^2\rangle(\mathbf{x}+\mathbf{r}) = 2\langle u_i^2\rangle(\mathbf{x}). \tag{27}$$

The second-order structure function and hence decay term do not depend on the spatial orientation. This is valid at both small separations (in locally isotropic regions of the flow), and at large scales, when Taylor's hypothesis is used. Large-scale anisotropies and inhomogeneities, which indeed exist in any flow, are not felt in the decay term.

Note that second-order structure functions are also included in the dissipative term, for which local isotropy has already been supposed. As this dissipative term explicitly depends on the second-order derivative with respect to r of the second-order structure function, it contains no information about the large-scale behavior of this structure function. In other words, the requirement that the decay term does not depend on the spatial orientation of the separation vector $\mathbf{r}$ is much stronger than imposing isotropy for the dissipative term, since these terms act over nonoverlapping ranges of scales. A similar analysis could be done for the third-order structure functions $\langle u_3(\Delta u_i)^2\rangle(\mathbf{r})$. For large scales, the limits of these functions are the same irrespectively of the orientation, when Taylor's hypothesis is used. For small scales, local isotropy imposes the same values of derivatives along any spatial direction. For intermediate scales, the structure functions behave in similar fashion.

Since all the terms in (22) depend on r only, we finally obtain by following the same procedure as in Ref. 33 and using the stationarity of this flow in a fixed laboratory reference frame

$$\begin{aligned}-\langle\Delta u_1(\Delta u_i)^2\rangle + 2\nu\frac{d}{dr}\langle(\Delta u_i)^2\rangle - \frac{1}{r^2}\int_0^r s^2[U_1\partial_1\langle(\Delta u_i)^2\rangle \\ + \partial_3\langle(u_3+u_3^+)(\Delta u_i)^2\rangle]ds = \frac{4}{3}\langle\epsilon\rangle r, \end{aligned} \tag{28}$$

where s is a dummy variable.

An important remark needs to be done at this stage. Both supplementary terms in Eq. (28) reflect a large-scale inhomogeneity in this fixed frame; the first, along the streamwise direction x_1, and the second along the direction x_3 normal to the wall. Further, in order to distinguish between the two terms, $U_1\partial_1\langle(\Delta u_i)^2\rangle$ reflects an inhomogeneity caused by the decay of the turbulence, whereas $\partial_3\langle(u_3+u_3^+)(\Delta u_i)^2\rangle$ is an inhomogeneity along the direction normal to the wall.

Equation (28) could be written in a dimensionless form as

$$A^* + B^* + \mathrm{INH1}^* + \mathrm{INH3}^* = C^*,$$

where $C^* = 4/3r^*$, INH1* is the inhomogeneous term along the streamwise direction x_1 and INH3* is the inhomogeneous term along the direction normal to the wall.

Note here the particular character of these inhomogeneous terms. They depend on particular flow directions (x_1 and x_3), so changing one of these directions will alter the result. From this point of view, they are not isotropic. Alternatively, when estimated via Taylor's hypothesis, they depend on r only, so they are used in a quasi-locally-isotropic frame.

Relation (28) is generally valid for all scales in any nearly locally isotropic flow or flow region such as:

(1) grid turbulence, where $U_1\partial_1\langle\ \rangle$ is the only extra term relative to the classical Kolmogorov equation terms,

(2) centerline of a channel flow, where the extra term is $\partial_3\langle\ \rangle$,

(3) centerline of a plane jet flow, where both $U_1\partial_1\langle\ \rangle$ and the lateral turbulent diffusion term need to be retained.

III. THE EFFECT OF THE LARGE-SCALE INHOMOGENEITY IN GRID TURBULENCE

In grid turbulence, it is well-known that the streamwise inhomogeneity (or decay) term plays a major role in balancing Eq. (28), whereas the inhomogeneities in a plane orthogonal to the flow direction are negligible. The previous analytical considerations retained the large scales influence, while simultaneously applying the concepts of local homogeneity and isotropy to scales much smaller than those at which injection occurs.

In grid turbulence, Eq. (28) reads

$$-\langle \Delta u_1(\Delta u_i)^2\rangle + 2\nu\frac{d}{dr}\langle(\Delta u_i)^2\rangle - \frac{U_1}{r^2}\int_0^r s^2\partial_1\langle(\Delta u_i)^2\rangle ds = \frac{4}{3}\langle\epsilon\rangle r. \tag{29}$$

Similarly, Eqs. (1) and (3) could be generalized as[4]

$$-\langle(\Delta u_1)^3\rangle + 6\nu\frac{d}{dr}\langle(\Delta u_1)^2\rangle - 3\frac{U_1}{r^4}\int_0^r s^4\partial_1\langle(\Delta u_1)^2\rangle ds = \frac{4}{5}\langle\epsilon\rangle r, \tag{30}$$

and

$$-\langle \Delta u_1(\Delta\theta)^2\rangle + 2\kappa\frac{d}{dr}\langle(\Delta\theta)^2\rangle - \frac{U_1}{r^2}\int_0^r s^2\partial_1\langle(\Delta\theta)^2\rangle ds = \frac{4}{3}\langle\epsilon_\theta\rangle r. \tag{31}$$

In (29), (30), and (31), s is a dummy variable. These equations may be written symbolically as $A+B+\mathrm{INH1}=C$, where C is proportional to the separation r and INH1 represents the streamwise inhomogeneous term.

We briefly assess here Eqs. (30) and (31) in the context of measurements downstream of a grid. Figure 2[4] shows that the influence of the inhomogeneous term in Eq. (30) is quite important, since the balance between $(4/5)r^*$ and the sum of the three normalized terms $A^*+B^*+\mathrm{NH1}^*$ is satisfactory for the whole range of separations, thus underlining the fact that the large scale streamwise inhomogeneity cannot be ignored in this type of flow.

Traditionally, it is argued that departures from the ''four-fifths law'' are attributed to a lack of isotropy. This work reassesses this argument. Even in locally isotropic flows, such as grid turbulence, Kolmogorov's or Yaglom's relations are not satisfied, at moderate Reynolds numbers. In order to balance these equations, the large-scale inhomogeneity needs to be properly considered. Only when estimating these inhomogeneous terms using Taylor's hypothesis could our new terms be treated in a quasi-isotropic context, i.e., using relation (24). Caution is therefore required when interpreting the observed departure from the ''four-fifths law'' in terms of a lack of local isotropy at moderate Reynolds numbers.

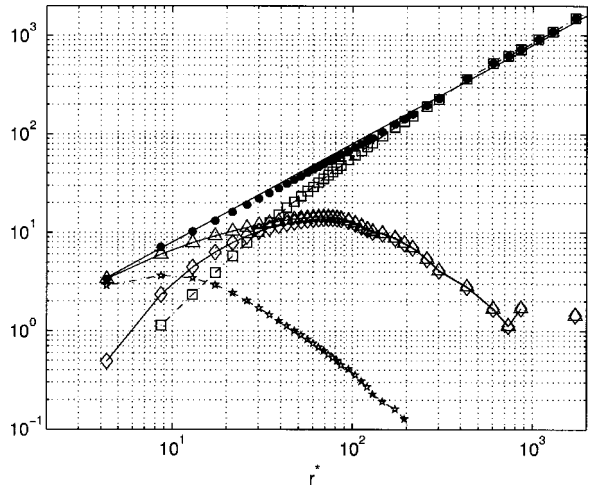

FIG. 2. Terms in the generalized Kolmogorov equation (30). (◇) A^*; (⋆) B^*; (△) A^*+B^*; (□) INH1*. $A^*+B^*+\mathrm{INH1}^*$ (●) is to be compared with C^* (solid line).

The data of Mydlarski and Warhaft were made available for a large range of R_λ (99–448) and allow to be checked against Eq. (30). Figure 3 shows the balance of Eq. (30) for two Reynolds numbers (99 and 448). The new term has a markedly stronger influence on inertial range (IR) scales when R_λ is smaller. Agreement between Eq. (30) and all the data sets is very well satisfied for all the investigated Reynolds numbers.

The same kind of analysis can be performed for the passive scalar field.[4] Scalar fluctuations were generated by means of a ''mandoline'' [32] placed downstream of the grid.

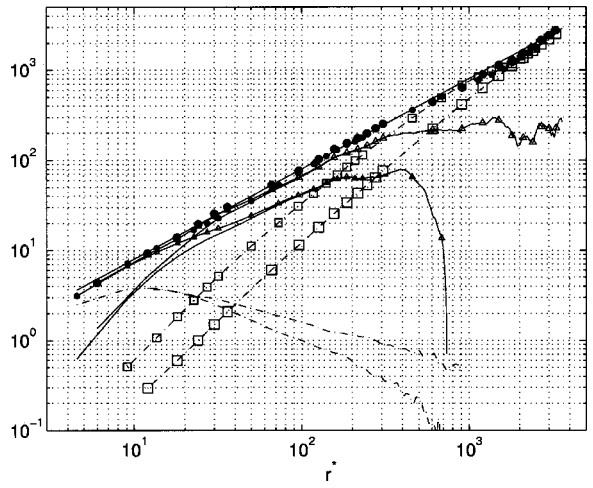

FIG. 3. Terms in Eq. (30) for Mydlarski and Warhaft's data. (—) A^*; —., B^*; (Δ and solid line), A^*+B^*; (solid line) C^*; (□) INH1*; $A^*+B^*+\mathrm{INH1}^*$, (● and solid line). $R_\lambda=99$: smaller symbols; $R_\lambda=448$: bigger symbols.

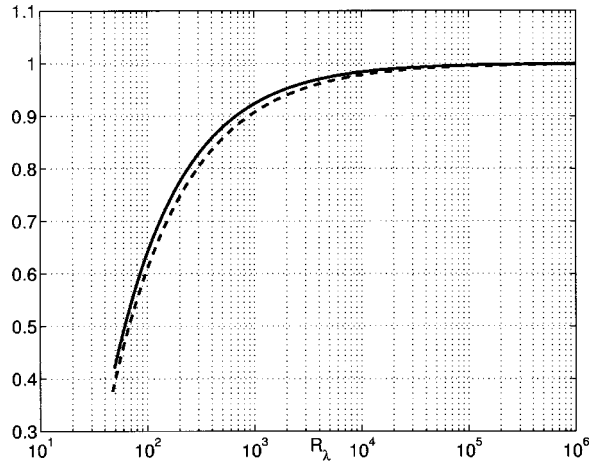

FIG. 4. Comparison between R_λ dependencies of the theoretical estimations in grid turbulence of $\langle(\Delta u_1)^3\rangle_t/(4/5\langle\epsilon\rangle r)$ (---) and $\langle\Delta u_1(\Delta\theta)^2\rangle_t/(4/3\langle\epsilon_\theta\rangle r)$ (—). The third-order moments are obtained from Eqs. (30) and (31).

The same level of agreement ($\pm 10\%$) was obtained between measurements and Eq. (31).

It is also worth examining the limiting trends of relations (29)–(31) at very large r. In this case, typically for $r>L$, $-\langle\Delta u_1(\Delta\theta^2)\rangle$ tends to zero and $\langle(\Delta\theta)^2\rangle$ asymptotes to $2\theta'^2$, so that the well-known decay law (e.g., Ref. 36) for the temperature variance is retrieved, viz.

$$U_1\frac{d}{dx_1}\langle\theta^2\rangle/2=-\langle\epsilon_\theta\rangle. \tag{32}$$

Similarly, Eq. (29) reduces to

$$U_1\frac{d}{dx_1}\langle u_i u_i\rangle/2=-\langle\epsilon\rangle. \tag{33}$$

The large-scale limiting behavior of Eq. (31) was discussed in more detail in Ref. 4. Equations (30) and (31) could be used to provide theoretical estimates of the third-order structure functions, i.e., $\langle(\Delta u_1)^3\rangle_t$ and $\langle\Delta u_1(\Delta\theta)^2\rangle_t$, in grid turbulence, over a range of values for R_λ. The second-order structure functions are either measured, or estimated (for large R_λ) with the use of Batchelor-type parametrization.[37,38] Figure 4 suggests that the ''4/5'' is first reached with a 1% accuracy, when R_λ exceeds 40 000, while ''4/3'' is attained at a somewhat slightly smaller value of R_λ.

Another generalized form of Yaglom's equation has been obtained in grid turbulence with a mean temperature gradient.[6,7] Temperature fluctuations are created by the mean temperature gradient, **G**, which exists in the x_3 direction. The effects of both the turbulent production of temperature fluctuations and the inhomogeneity downstream of the (active) grid have been taken into account.[39] The result is a generalized form of Yaglom's equation that contains additional terms resulting from **G** and the streamwise inhomogeneity:

$$-\langle\Delta u_1(\Delta\theta)^2\rangle+2\kappa\frac{d}{dr}\langle(\Delta\theta)^2\rangle-\frac{1}{r^2}\int_0^r s^2[U_1\partial_1\langle(\Delta\theta)^2\rangle + 2G\langle\Delta u_3\Delta\theta\rangle]ds=\frac{4}{3}\langle\epsilon_\theta\rangle r, \tag{34}$$

where $G=|\mathbf{G}|$. Agreement between the theory and experiment is adequate and the effects from the strictly inhomogeneities in the flow are small. In Ref. 4, the scalar field is locally isotropic and the streamwise inhomogeneity is the only large-scale mechanism in this flow. Consequently, the streamwise inhomogeneity (or the decay) dominates the generalized Yaglom equation at large scales. The study of grid turbulence with mean-temperature gradient involves two large-scale mechanisms (production and streamwise inhomogeneity). This, together with the small-scale anisotropy arising from the mean-temperature gradient, resulted[39] in a less accurate balance of Eq. (34) than obtained in Ref. 4.

It is worth noting that Eqs. (30) and (31) also reproduce at small r the rates of decay of $\langle\epsilon\rangle$ and $\langle\epsilon_\theta\rangle$, as represented by (for locally isotropic turbulence)[40]

$$-\frac{U_1}{35\nu}\frac{d\langle\epsilon\rangle}{dx_1}=\left\langle\left(\frac{\partial u_1}{\partial x_1}\right)^3\right\rangle+2\nu\left\langle\left(\frac{\partial^2 u_1}{\partial x_1^2}\right)^2\right\rangle, \tag{35}$$

$$-\frac{U_1}{15\kappa}\frac{d\langle\epsilon_\theta\rangle}{dx_1}=\left\langle\frac{\partial u_1}{\partial x_1}\left(\frac{\partial\theta}{\partial x_1}\right)^2\right\rangle+2\frac{\kappa}{3}\left\langle\left(\frac{\partial^2\theta}{\partial x_1^2}\right)^2\right\rangle. \tag{36}$$

These transport equations correspond to those derived by Batchelor and Townsend[41] and Corrsin.[42] We note that (35) and (36) are obtained by equating terms of order r^3 after writing Taylor series expansions for $\langle(\Delta u_1)^2\rangle$ and $\langle(\Delta\theta)^2\rangle$, in the limit of $r\to 0$. The appearance of the inhomogeneous terms in Eqs. (30) and (31) is thus fully consistent with the streamwise inhomogeneity of $\langle\epsilon\rangle$ and $\langle\epsilon_\theta\rangle$ for this particular flow. Evidently, this feature cannot be reproduced by the classical Eqs. (1) and (3).

IV. THE EFFECT OF THE LATERAL DIFFUSION ON THE CENTERLINE OF A CHANNEL FLOW

On the centerline of a fully developed channel flow, Eq. (28) becomes[30]

$$-\langle\Delta u_1(\Delta u_i)^2\rangle+2\nu\frac{d}{dr}\langle(\Delta u_i)^2\rangle - \frac{1}{r^2}\int_0^r s^2\partial_3\langle(u_3+u_3^+)(\Delta u_i)^2\rangle ds=\frac{4}{3}\langle\epsilon\rangle r, \tag{37}$$

which could be written as

$$A^*+B^*+\mathrm{INH3}^*=C^*.$$

Figure 5 displays all the terms in Eq. (37). While A^*, B^*, and C^* are obviously the same as in Eq. (1), the new term INH3* improves the balance over the restricted scaling range and, more particularly, for very large scales. The accuracy with which the new equation is satisfied is about $\pm 10\%$ in the range $r\gtrsim 20\eta$. Figure 6 shows the ratios of different terms in Eq. (37) with respect to C^*. The ratio $(A^*+B^*+\mathrm{INH3}^*)/C^*$ is within $\pm 10\%$ of the theoretical value of 1.

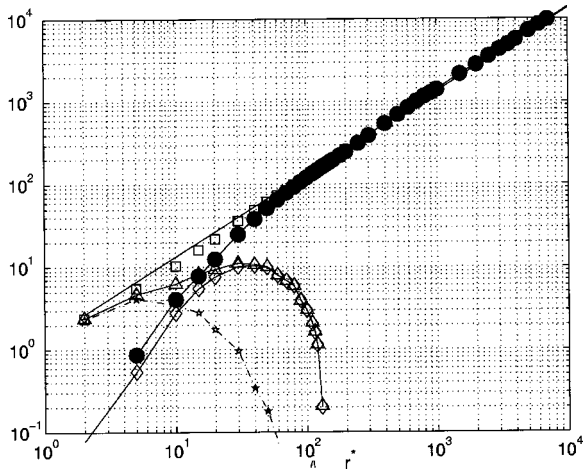

FIG. 5. Verification of Eq. (37), which includes an inhomogeneous term INH3: turbulent transport term A^* ($\diamond$ and —), small-scale diffusion term B^* (* and —), A^*+B^* (Δ and —), INH3 ($\bullet$ and —). $A^*+B^*+\mathrm{INH}^*$ ($\square$ and —) is to be compared with C^* (—).

This result clearly emphasizes the role played by the large-scale inhomogeneity in the budget equation, or the energy at a given scale.

Note that a generalized form of Yaglom's equation in a slightly heated channel flow should take into account both the presence of a mean temperature gradient as well as the large-scale inhomogeneity of the velocity field.

The limiting form, at very large scales, of this equation can be obtained by applying the same method as previously. The result is

$$\lim_{r\to\infty} \mathrm{INH3} = \lim_{r\to\infty} \frac{-2}{r^2} \int_L^r y^2 \partial_3 \langle u_3 (\Delta u_i)^2 \rangle dy$$

$$= -\frac{2r}{3} \partial_3 \langle u_3 u_i^2 \rangle = \frac{4}{3} \langle \epsilon \rangle r. \tag{38}$$

The kinetic energy balance equation, obtained from Navier–Stokes equations written in one-point, using homogeneity and only weak isotropy (pressure diffusion is neglected), then reduces on the channel centerline

$$\langle \epsilon \rangle = -\tfrac{1}{2} \partial_3 \langle u_3 u_i u_i \rangle, \tag{39}$$

where the strongest hypothesis used here is homogeneity. The generalized form of the extended Kolmogorov equation (37) is therefore consistent, at the very large scales, with relation (39). A quantitative comparison between different forms of $\langle \epsilon \rangle$ is given in Ref. 30.

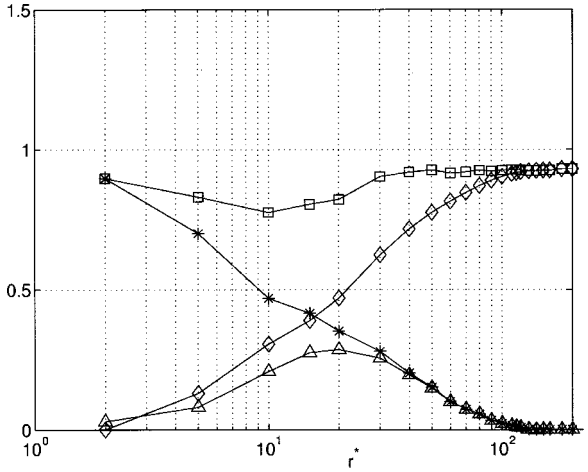

FIG. 6. Ratio of terms in Eq. (37) and C^*: A^*/C^* ($\triangle$ and —), $(A^*+B^*)/C^*$ (* and —), $\mathrm{INH3}^*/C^*$ ($\diamond$ and —) and $(A^*+B^*+\mathrm{INH3}^*)/C^*$ ($\square$ and —).

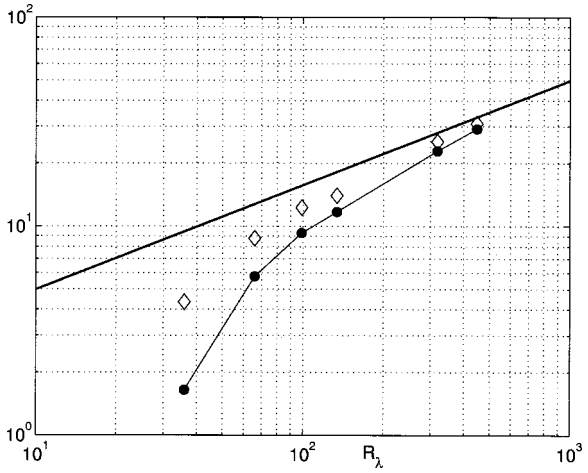

FIG. 7. R_λ dependence of values of terms A^*, A^*+B^* and C^* in Eq. (30), for $r=\lambda$. (Solid line and $\bullet$) $A^*_{r=\lambda}$; $\diamond$, $(A^*+B^*)_{r=\lambda}$; (solid line) term $C^*_{r=\lambda}$.

V. CONCLUDING REMARKS

Generalized forms of the equations of Kolmogorov and Yaglom have been proposed and verified in decaying grid turbulence and on the centerline of a fully developed turbulent channel flow. The new equations take into account the nonhomogeneities of the large scales, which act either along the streamwise direction (grid turbulence), or in a direction normal to the wall (channel flow). An interesting aspect of the equations is that they essentially represent budget equations for the energy at different scales.

Taking account of the large-scale inhomogeneity results in a significant improvement of the budget, the level of agreement being typically about $\pm 10\%$ over the full range of scales. In order to better emphasize the role played by the large-scale (streamwise or transverse) inhomogeneity, we plot in Fig. 7 the values of the "classical" terms in Eq. (1) for $r=\lambda$, near the bottom end of the RSR. In Fig. 7 six Reynolds numbers have been used, specific to the data analyzed here. The smallest R_λ ($=36$) corresponds to the centerline of a fully developed channel flow (Ref. 30, and Sec. IV of this paper). The other five values of R_λ are associated with measurements in decaying grid turbulence (Refs. 4 and 6, and Sec. III of this paper). The viscous/molecular contribution (e.g., term B^*, or the difference between diamonds and closed circles in Fig. 7) is non-negligible at this scale for moderate Reynolds numbers. As was pointed out previously, the inhomogeneous contributions (the difference between the solid line and the diamond) is more important than the vis-

cous term at $R_\lambda = 36$; it has approximately the same importance as the viscous term at the other Reynolds numbers. Thus, viscous effects, turbulent advection, and large-scale nonhomogeneities need to be properly considered in the transport equations of second-order moments.

Our equations do not contradict the classical relations in Kolmogorov's theoretical framework; they simply extend them, at least in a few particular situations. Equations (1) and (3) are clearly obtained by supposing local isotropy and homogeneity in high Reynolds numbers flows. For very small scales, our Eqs. (29), (30), and (31) lead to isotropic or homogeneous definitions of $\langle \epsilon \rangle$ given by (7), (9), and (11). Much more importantly, as shown in Secs. III and IV, our equations, when analyzed using one-point measurements and Taylor's hypothesis, are, at very large scales, consistent with different expressions of $\langle \epsilon \rangle$ (or $\langle \epsilon_\theta \rangle$) obtained from the Navier–Stokes equations (or the heat transfer equation), viz. Eqs. (32), (33), and (39). These equations, which are kinetic energy budget equations written for different flows or different flow regions, have been known for some time now.[43] It was straightforward to note that the two-point energy budget equations, i.e., the equations of Kolmogorov and Yaglom, when estimated using one-point temporal measurements and Taylor's hypothesis should reduce, at very large separations (when the two points become decorrelated), to the one-point energy budget equations.

The generalized equations (29)–(31) are simply a ''bridge'' between the already known forms of these equations, e.g., Eqs. (1) and (3) and the (also already known) one-point energy budget equations; this represents the main contribution of our work. Note also that the success of the new equations was achieved in flows or flow regions where the isotropic forms of $\langle \epsilon \rangle$ (i.e., the small-scale limits of our equations) are very close to the values of $\langle \epsilon \rangle$ given by the one-point energy budget (i.e., the large-scale limits of our equations). We therefore expect a lower quality of agreement when a mean shear is present. This aspect needs further investigation.

There is a need to distinguish between our work and that of Lindborg.[18] We use different forms of nonhomogeneities adapted to each flow (our term INH1 is different from INH3). These terms depend on different structure functions, for instance $\langle (\Delta u_1)^2 \rangle$ for INH1 and $\langle u_3 (\Delta u_i)^2 \rangle$ for INH3 with different scaling behaviors. We also use experimentally determined values for $\langle \epsilon \rangle$. Lindborg wrote a generalized form of the Kolmogorov equation [our Eq. (30)], but uses the $k-\epsilon$ model for determining the mean dissipation rate thus ''forcing'' the balance of this equation at very large scales by optimizing the constants in the model. Further, he only uses the second-order structure function $\langle (\Delta u_1)^2 \rangle$ in order to infer a quantitative value of the source term, irrespectively of the flow. This leads to inferior agreement of the written equation in the RSR. We finally underline that each flow needs to be treated separately, by taking into account its own physical characteristics and mathematically translating these into appropriate expressions for structure functions.

Our results indicate that, for moderate Reynolds numbers, the third-order structure function is not well-adapted (as traditionally thought) to defining an inertial range since it does not scale with r. Its value does not balance $4/5\langle \epsilon \rangle r$ and it does not lead to a good estimation of $\langle \epsilon \rangle$. Large-scale inhomogeneity also needs to be considered. This shortcoming of the third-order structure function has been associated with the so-called ''finite Reynolds number'' (FRN) effect by Qian.[44] Quantifications of this effect were carried out using the ''exact spectral equations'' for two particular cases: freely decaying isotropic turbulence and shear flow turbulence. In the former case, the exact spectral equation is[45–48]

$$\frac{\partial E(k)}{\partial t} + 2\nu k^2 E(k) = T(k), \tag{40}$$

where k is the wave number modulus, $E(k)$ is the three-dimensional energy spectrum, and $T(k)$ is the energy transfer spectrum function. Equation (40), which has been known since 1948, is the spectral equivalent of Eq. (30): $T(k)$ is the equivalent of the third-order structure function (term A); $2\nu k^2 E(k)$ corresponds to both terms B and C, while $\partial E(k)/\partial t$ corresponds to the streamwise inhomogeneous term INH1. Strictly, the classical Kolmogorov equation (1) corresponds to Eq. (40) without the decaying term. Qian has written the third-order structure function using $T(k)$ [see his relation (7) and Ref. 33], which is further written [using (40)] in terms of a viscous contribution (his term G_2) and especially a term (G_1) which represents the ''energy input at large scales.'' Different models are used for this last function, finally leading to the estimation of the FRN effect through the third-order structure function. For decaying isotropic turbulence, Qian's treatment is identical to ours,[4] although he avoids the use of physical space, preferring to remain in the spectral domain. Qian also addresses the case of a mean shear but does not consider flow regions such as the centerline of a fully developed channel flow where neither turbulence decay nor shear are present. An important example of the present work is to investigate those regions of the flow which are not locally isotropic, for example, the region near the wall. The spectral domain may arguably be the better way of characterizing these regions, through simpler mathematical calculations.

Given that, at Reynolds numbers normally encountered in the laboratory, the third-order moment (term A) cannot be proportional to r over a large range of scales, it is worth enquiring if term A can continue to be used for determining the inertial range. The scales over which $A \propto r$ are then ''restricted'' and we thus refer to a restricted scaling range RSR. In this RSR, one could determine the scaling exponents ζ_n (defined as $S_n = \langle (\Delta \alpha)^n \rangle \propto r^{\zeta_n}$, where α represents either u_1 or θ), and compare them with Kolmogorov's predictions. It is now generally accepted that an unambiguous estimation of ζ_n is fraught with difficulties. While the ESS method (Ref. 49) avoids some of these, it lacks a sound theoretical basis.

Large scale inhomogeneities have to be taken into account in analytical intermittency studies.[18] It is now clear that the behavior of the third-order moment is ''shaped'' by both viscous and large-scale effects. Similarly, the large-scale inhomogeneity plays a role in the budget equations for nth order moments (for example, $S_n \equiv \langle (\Delta \theta)^n \rangle$) derived from the advection–diffusion equation in similar fashion to

Yaglom's equation. In grid turbulence heated by a mandoline, this inhomogeneity is $\partial S_n/\partial t$, while, in all the other flows, the ''source term'' is much more complicated. Understanding how the advection–diffusion equation ''creates'' the intermittency, is an important problem,[50] which has only been solved for rather particular conditions. The correct behavior of S_n is described by a more complete equation which should also consider the inhomogeneity specific to the flow.

The aim of our work was to correctly describe the behavior of the third-order moments in particular flows, and to ensure that all physical phenomena specific to the flow are taken into account. A future objective will be to consider the energy budget equations on the axis of a round jet, where there are both streamwise and lateral inhomogeneities.

ACKNOWLEDGMENTS

R.A.A. acknowledges the support of the Australian Research Council. The authors are most grateful to Dr. T. Zhou for providing his grid turbulence and channel flow data.

[1] A. N. Kolmogorov, ''The local structure of turbulence in incompressible viscous fluid for very large Reynolds numbers,'' Dokl. Akad. Nauk SSSR **30**, 301 (1941).
[2] A. N. Kolmogorov, ''Dissipation of energy in locally isotropic turbulence,'' Dokl. Akad. Nauk SSSR **32**, 16 (1941).
[3] A. M. Yaglom, ''On the local structure of a temperature field in a turbulent flow,'' Dokl. Akad. Nauk SSSR **69**, 743 (1949).
[4] L. Danaila, F. Anselmet, T. Zhou, and R. A. Antonia, ''A generalization of Yaglom's equation which accounts for the large-scale forcing in heated decaying turbulence,'' J. Fluid Mech. **391**, 359 (1999).
[5] R. A. Antonia, A. J. Chambers, and L. W. Browne, ''Relations between structure functions of velocity and temperature in a turbulent jet,'' Exp. Fluids **1**, 213 (1983).
[6] L. Mydlarski and Z. Warhaft, ''On the onset of high Reynolds number grid generated wind tunnel turbulence,'' J. Fluid Mech. **320**, 331 (1996).
[7] L. Mydlarski and Z. Warhaft, ''Passive scalar statistics in high-Péclet-number grid turbulence,'' J. Fluid Mech. **358**, 135 (1998).
[8] B. Pearson and R. A. Antonia, ''Reynolds number dependence of turbulent velocity and pressure increments,'' J. Fluid Mech. **444**, 343 (2001).
[9] R. A. Antonia, ''Reynolds number dependence of velocity and temperature increments in turbulent flows,'' Third International Symposium of Turbulence, Heat and Mass Transfer, edited by Y. Nagano, K. Hanjalic, and T. Tsuji, 2000, p. 3.
[10] J. Jiménez, A. A. Wray, P. G. Saffman, and R. Rogallo, ''The structure of intense vorticity in isotropic turbulence,'' J. Fluid Mech. **255**, 65 (1993).
[11] T. Gotoh and R. Rogallo, ''Intermittency and scaling of pressure at small scales in forced isotropic turbulence,'' J. Fluid Mech. **396**, 257 (1999).
[12] T. Gotoh (private communication).
[13] O. N. Boratav and R. B. Pelz, ''Structures and structure functions in the inertial range of turbulence,'' Phys. Fluids **9**, 1400 (1997).
[14] K. Alvelius, ''Random forcing of three-dimensional homogeneous turbulence,'' Phys. Fluids **11**, 1880 (2000).
[15] U. Frisch, *Turbulence: The Legacy of A. N. Kolmogorov* (Cambridge University Press, Cambridge, 1995).
[16] R. J. Hill, ''Applicability of Kolomogorov's and Monin's equations of turbulence,'' J. Fluid Mech. **353**, 67 (1997).
[17] F. Moisy, P. Tabeling, and H. Willaime, ''Kolmogorov equation in a fully developed turbulence experiment,'' Phys. Rev. Lett. **82**, 3994 (1999).
[18] E. Lindborg, ''Corrections to the four-fifths law due to variations of the dissipation,'' Phys. Fluids **11**, 510 (1999).
[19] P. A. Durbin and C. G. Speziale, ''Local anisotropy in strained turbulence at high Reynolds numbers,'' in *Recent Advances in Mechanics of Structured Continua*, edited by M. Massoudi and K. R. Rajagopal (American Society of Mechanical Engineers, New York, 1991), AMD-117, p. 29.
[20] X. Shen and Z. Warhaft, ''The anisotropy of the small-scale structure in high-Reynolds number ($R_\lambda \approx 1000$) turbulent shear flow,'' Phys. Fluids **12**, 2976 (2000).
[21] M. Ferchichi and S. Tavoularis, ''Reynolds number effects on the fine structure of uniformly sheared turbulence,'' Phys. Fluids **12**, 2942 (2000).
[22] K. R. Sreenivasan, ''On local isotropy of passive scalars in turbulent shear flows,'' Proc. R. Soc. London, Ser. A **434**, 165 (1991).
[23] C. Tong and Z. Warhaft, ''On passive scalar derivative statistics in grid turbulence,'' Phys. Fluids **6**, 2165 (1994).
[24] A. Pumir, ''A numerical study of the mixing of the passive scalar in three dimensions in the presence of a mean gradient,'' Phys. Fluids **6**, 2118 (1994).
[25] M. Holzer and E. D. Siggia, ''Turbulent mixing of a passive scalar,'' Phys. Fluids **6**, 1820 (1994).
[26] R. A. Antonia, M. Ould-Rouis, F. Anselmet, and Y. Zhu, ''Analogy between predictions of Kolmogorov and Yaglom,'' J. Fluid Mech. **332**, 395 (1997).
[27] R. A. Antonia and B. R. Pearson, ''Effect of initial conditions on the mean energy dissipation rate and the scaling exponent,'' Phys. Rev. E **62**, 8086 (2000).
[28] G. Xu, R. A. Antonia, and S. Rajagopolan, ''Scaling of mean temperature dissipation rate,'' Phys. Fluids **12**, 3090 (2000).
[29] J. L. Lumley, ''Some comments on turbulence,'' Phys. Fluids A **4**, 203 (1992).
[30] L. Danaila, F. Anselmet, T. Zhou, and R. A. Antonia, ''Turbulent energy scale-budget equations in a fully developed channel flow,'' J. Fluid Mech. **430**, 87 (2001).
[31] A. Sirivat and Z. Warhaft, ''The effect of a passive cross-stream temperature gradient on the evolution of temperature variance and heat flux in grid turbulence,'' J. Fluid Mech. **128**, 323 (1983).
[32] Z. Warhaft and J. L. Lumley, ''An experimental study of the decay of temperature fluctuations in grid generated turbulence,'' J. Fluid Mech. **88**, 659 (1978).
[33] A. S. Monin and A. M. Yaglom, *Statistical Fluid Mechanics* (MIT, Cambridge, 1975), Vol. 2.
[34] J. Kim, P. Moin, and R. Moser, ''Turbulence statistics in fully developed channel flow at low Reynolds numbers,'' J. Fluid Mech. **177**, 133 (1987).
[35] N. N. Mansour, J. Kim, and P. Moin, ''Reynolds-stress and dissipation rate budgets in a turbulent channel flow,'' J. Fluid Mech. **194**, 15 (1988).
[36] L. Danaila, F. Anselmet, T. Zhou, and R. A. Antonia, ''Calibration of a temperature dissipation probe in decaying turbulence,'' Exp. Fluids **28**, 45 (2000).
[37] R. A. Antonia, T. Zhou, and G. Xu, ''Second-order temperature and velocity structure functions: Reynolds number dependence,'' Phys. Fluids **12**, 1509 (2000).
[38] T. Zhou, R. A. Antonia, L. Danaila, and F. Anselmet, ''Approach to the four-fifths 'law' for grid turbulence,'' J. Turbulence **1**, 5 (2000).
[39] L. Danaila and L. Mydlarski, ''The effect of gradient production on scalar fluctuations in decaying grid turbulence,'' Phys. Rev. E **64**, 016316 (2001).
[40] T. Zhou, R. A. Antonia, L. Danaila, and F. Anselmet, ''Transport equations for the mean energy and temperature dissipation rates in grid turbulence,'' Exp. Fluids **28**, 143 (2000).
[41] G. K. Batchelor and A. A. Townsend, ''Decay of vorticity in isotropic turbulence,'' Proc. R. Soc. London, Ser. A **190**, 534 (1947).
[42] S. Corrsin, ''Heat transfer in isotropic turbulence,'' J. Appl. Phys. **23**, 113 (1952).
[43] A. A. Townsend, *The Structure of Turbulent Shear Flow* (Cambridge University Press, Cambridge, 1976).
[44] J. Qian, ''Slow decay of the finite Reynolds number effect of turbulence,'' Phys. Rev. E **60**, 3409 (1999).
[45] C. C. Lin, ''Note on the law of decay of isotropic turbulence,'' Proc. Natl. Acad. Sci. USA **34**, 230 (1948).
[46] A. A. Townsend and G. K. Batchelor, ''Decay of turbulence in the final period,'' Proc. R. Soc. London, Ser. A **194**, 1039 (1948); **194**, 527 (1948).
[47] H. Tennekes and J. Lumley, *First Course in Turbulence* (MIT, Cambridge, 1974).
[48] M. S. Uberoi, ''Energy transfer in isotropic turbulence,'' Phys. Fluids **6**, 1048 (1963).
[49] R. Benzi, S. Ciliberto, R. Tripiccione, C. Baudet, and S. Succi, ''Extended self-similarity in turbulent flows,'' Phys. Rev. E **48**, 29 (1993).
[50] R. H. Kraichnan, ''Anomalous scaling of a randomly advected passive scalar,'' Phys. Rev. Lett. **72**, 1016 (1994).